JOURNAL OF MATERIALS SCIENCE 20 (1985) 3621–3630

Adhesion to skin

Part 1 *Peel tests with hard and soft machines*

E. H. ANDREWS, T. A. KHAN, H. A. MAJID
Department of Materials, Queen Mary College, Mile End Road, London E1 4NS, UK

A modified adhesive peel test is described in which a spring is inserted between the test machine cross-head and the peeling strip. In tests using two pressure sensitive surgical adhesives (uncrosslinked elastomers) this "soft machine" gives results which differ significantly from those obtained with a conventional "hard machine". In particular, when peeling energy is plotted against peeling velocity, the soft machine reveals a regime of low energy peeling and a transition to the normal high energy peeling. The transition behaviour has been studied as a function of adhesive thickness, cross-head speed and spring stiffness. The phenomena revealed by soft machine testing are interpreted in terms of variations in crack-tip radius caused by flow of the uncrosslinked rubber. The practical implication is that far more information can be obtained from soft machine tests than from conventional hard machine tests. The problem of oscillating peel force is also eliminated.

1. Introduction

Peel testing is a convenient method of assessing adhesive strength when one or both of the adherends are flexible. There is a further advantage that the peeling force converts simply to the adhesive failure energy per unit area, θ, by the formula [1]

$$\theta = P(1 - \cos\gamma)/b \qquad (1)$$

where b is the width of the peeling strip and γ is the peel angle. Equation 1 assumes, of course, that energy storage and dissipation in the peeled portion of the specimen is negligible and this assumption is not always justified [2]. There is an extensive literature on peel testing which will not be reviewed here because it is widely known. Some useful sources of information are given, however, in [3–6].

The work described in this paper concerns the adhesion of polymeric adhesives to human skin and has as its ultimate objective the improvement of adhesive wound-dressings and related products. The adhesives studied were commercial products based upon uncrosslinked elastomeric polymers.

Uncrosslinked materials are capable of flow and their adhesive behaviour is considerably more complex than that of crossslinked elastomers. Crosslinked adhesives have been studied extensively [7–12] and their peeling energy can be separated into two components according to the equation [7, 13],

$$\theta = \theta_0 \Phi(\dot{c}, T, \varepsilon_0) \qquad (2)$$

where θ_0 is the interfacial bond energy (equal to the thermodynamic work of adhesion if there is no primary interfacial bonding) and Φ is a loss function depending on velocity $\dot{c}$, temperature T and strain ε_0. Equation 2 was first derived mathematically by Andrews and Kinloch [7], but the separability of interfacial and bulk contributions to adhesive strength was originally predicted by Gent and Schultz [8] on the basis of experiments in which peeling tests were carried out under various liquids.

Some authors have pointed out that peel tests on crosslinked elastomers do not necessarily give simple separability of the bulk and interfacial components [14, 15] but it is important to realize that Equation 2 does not predict simple

0022–2461/85 $03.00 + .12

factorization of θ unless Φ is independent of the applied strain ε_0. In many cases this independence is found and curves of $\log\theta$ against $\log\dot{c}$ are parallel for different θ_0. At high peeling loads, low peeling angles or at temperatures close to T_g of the adhesive, however, Φ frequently becomes strain (or stress) dependent and curves for different θ_0 are no longer parallel.

A related observation is that time–temperature superposition of plots of $\log\theta$ against $\log\dot{c}$ will only be obtained if the energy losses encompassed by the loss function Φ are thermorheologically simple. If dissipative processes occur that are not linearly viscoelastic in nature, then Equation 2 remains valid, but Φ is not uniquely determined by the reduced velocity $\dot{c}a_T$ (where a_T is the WLF shift factor).

At very low peeling velocities $\Phi \rightarrow 1$ for unfilled crosslinked elastomers and it is possible in principle to observe a region where θ becomes independent of rate and temperature and assumes the value θ_0. In practice it is very difficult to access this region experimentally since peeling rates are so small and since oxidative attack may occur on the same time-scale as peeling. There is, however, an alternative method of obtaining θ_0.

Since Φ is a property of the bulk phase it also controls the cohesive failure of the elastomer, thus:

$$\mathscr{T} = \mathscr{T}_0 \Phi(\dot{c}, T, \varepsilon_0) \qquad (3)$$

where $\mathscr{T}$ is the bulk fracture energy and $\mathscr{T}_0$ the cohesive energy per unit area of the solid. Dividing Equation 2 by Equation 3 we obtain

$$\theta = \theta_0(\mathscr{T}/\mathscr{T}_0) \qquad (4)$$

provided the dependence of Φ upon strain can be ignored. Thus a knowledge of $\mathscr{T}_0$ (which can be calculated [16, 17] or measured by limiting fatigue testing [18] enables θ_0 to be deduced from the measured values of θ and $\mathscr{T}$ [7].

When we turn to uncrosslinked elastomers (and other pressure sensitive adhesives) the situation is more complex. Experimental work on such systems has been published by several authors [19, 22] and a general pattern of behaviour has emerged.

At low peeling rates failure is cohesive (failure *within* the adhesive phase) with peeling energy θ increasing with rate. At a critical peeling rate, which depends upon temperature, molecular weight and material, a rapid transition occurs to adhesive failure (failure at the interface). This transition can be ascribed to the suppression of molecular flow in the adhesive which then exhibits the higher strength behaviour of an entanglement network. Such a network does not have time to relax at the higher rates of deformation. This is not the whole story, however, since peeling energy often *falls* at this transition and this cannot be explained simply by a change in the locus of failure from bulk to interface but must also involve a change in the mechanism of rheological energy dissipation.

Some authors have demonstrated that time–temperature superposition is possible in plots of $\log\theta$ against $\log\dot{c}$ [20, 21] although our experience is that the cohesive–adhesive transition does not necessarily superimpose along with the cohesive or adhesive regions of the curve. The master curves obtained by superposition exhibit the following general regions [21].

(a) Cohesive failure at low $\dot{c}$, θ rising with $\dot{c}$.

(b) Cohesive → adhesive transition, θ may fall sharply.

(c) Adhesive failure, θ increasing with $\dot{c}$. Failure is fibrillar.

(d) Adhesive failure, θ falling with $\dot{c}$. Failure is "glassy".

The transition (c) → (d) can be viewed as a glass transition phenomenon.

In spite of this overall phenomenological pattern, it is clear that the peel behaviour of uncrosslinked elastomers is not fully defined. We have found, for example, that a natural rubber-based adhesive exhibits no drop in peeling energy at the cohesive–adhesive transition, whereas acrylic adhesives show a large drop in θ. A further problem commonly found in conventional peel testing is the unsteady magnitude of the peeling force, revealing time-dependent phenomena in the system which are not fully resolved by the test.

The novel test method described in this paper was adopted initially in an attempt to suppress the load oscillations which occur at higher peeling rates. It was thought that a more definitive value of peeling force might be obtained in this way. This suppression was indeed achieved but a number of new phenomena were also observed with the "soft machine" test which are not

obtained in conventional peel testing. These new effects provide fresh insights into the peel behaviour of uncrosslinked elastomers, the more so because they are fully quantitative. An added bonus is that a single test using the new technique provides the same information as a plurality of conventional peel experiments.

2. Testing procedures

All the work reported here used a peeling angle γ of 90°. To maintain this angle in machine tests, the specimen was mounted on a free-running trolley as shown in Fig. 1. The effect of the trolley is, of course, to keep the point of peel detachment directly underneath the point of load application.

Normal 90° peel testing (hard-machine testing) was carried out by attaching the peeling strip directly to the cross-head of a Table Model Instron machine. The new peel test method (soft-machine testing) was achieved by interposing a coil spring between the end of the peeling strip and the machine cross-head (Fig. 1).

In hard-machine tests the average rate of peeling is imposed by the cross-head which is driven at a constant rate $\dot{X}$. The peel strip responds by exerting a force P upon the load cell. Since, however, the peel strip does not necessarily "accept" the imposed steady rate of peeling, it may peel at variable rate and force in such a way as to match the average peeling rate imposed. Since the system is stiff, rapid oscillations may occur in the peel force P (see Fig. 2).

With a soft machine, the peel strip is not compelled to follow the cross-head but may peel at a rate (including zero rate) determined only by its adhesive properties and the instantaneous load.

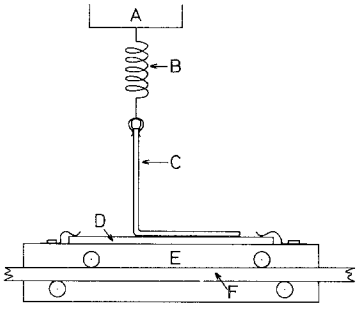

Figure 1 Soft-machine peel testing at 90° peel angle. A, cross-head; B, spring; C, peel strip; D, substrate; E, trolley; F, stationary bearer.

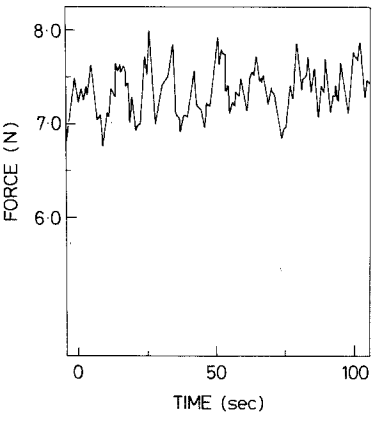

Figure 2 Typical hard-machine test result (NR at 50 mm min^{-1} cross-head speed with 2 cm wide peel strip).

The rate of peel, $\dot{c}$, is easily obtained from the force–time diagram since it is the difference between the cross-head speed $\dot{X}$ and the relative rate of displacement of the two ends of the spring. This assumes that the peeled portion of the specimen is inextensible, a condition that can always be ensured by using a high modulus backing material. Then, if L is the spring length,

$$\dot{c} = \dot{X} - (\mathrm{d}L/\mathrm{d}t) \qquad (2)$$
$$= \dot{X} - k(\mathrm{d}P/\mathrm{d}t)$$

where P is the peeling force and k the inverse spring constant ($P = k^{-1}\Delta L$). Thus the peeling rate at any load is given by the cross-head speed and the slope of the load–time curve at that point. Fig. 3 shows a typical load–time plot for soft-machine testing. The slopes were determined by hand but equipment has since been developed which digitizes the load signal and evaluates $\dot{c}$ by microprocessor. It is then possible for the computer to plot out directly a curve of θ against $\dot{c}$ (or $\log\theta$ against $\dot{c}$) using Equations 1 and 5.

Finally, to obtain very low speed peeling, some experiments were done using a dead-load 90° peel configuration in which the specimen was peeled from the underside of a glass plate by hanging a weight on its free end.

3. Materials, specimen preparation and testing conditions

Two proprietory commercial adhesives, supplied by Smith and Nephew Ltd, were employed. The natural-rubber based material (NR) was a surgical adhesive conforming to BP specification

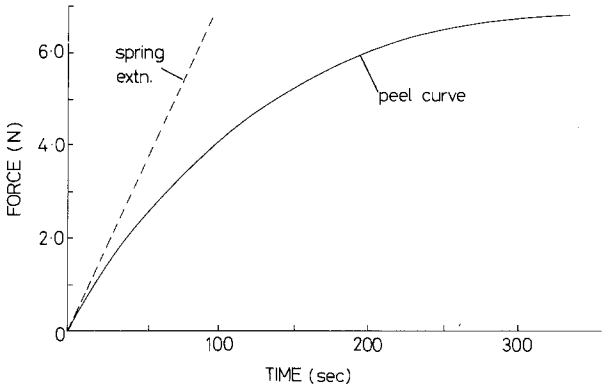

Figure 3 Typical soft-machine test result. (Details as for Fig. 2.)

and containing natural rubber, colophony resin, lanolin and zinc oxide.

The acrylic rubber adhesive (AR) was a surgical grade acrylic adhesive prepared according to British Patent 2 070 631.

To prepare specimens, solutions of the adhesives were spread on a backing of cotton cloth in such a way that the warp threads would lie in the pulling direction during peel testing. This ensures negligible extension of the peeling strip combined with effectively zero resistance to bending at the point of peel. The peeling strip was attached to the cross-head or the spring by means of a suitable clamp.

The weight of adhesive applied could be varied as follows. The adhesives/solvent mixture was poured into a rectangular box having a variable slit along one lower edge. This box was drawn slowly across the cotton cloth to deposit a uniform layer of material whose thickness was dependent upon the slit width.

The adhesive was allowed to dry at room temperature for 24 h before peel strips measuring 20 mm × 120 mm were cut out using a scalpel. For peel testing these strips were stuck down either to clean float glass (used as a reference substrate) or to skin (inner aspect of the forearm of a volunteer subject) and left for 1 min before testing.

In order to investigate the effects of absorbed skin secretions (sebum) on the adhesive properties, a proprietory artificial sebum composition was added to the adhesive/solvent mixtures in varying proportions by weight. Similarly, some of the major sebum constituents were added individually to the adhesives. Results from some of these preparations will be quoted in this paper but discussion of the effects of such additives will be reserved for a later publication. The tests with added sebum/lipids/fatty acids were all done using glass as the substrate.

Peel testing was carried out at various cross-head speeds and at various temperatures provided by a heated enclosure into which the forearm could be inserted. It should be realised that living skin substrates exert a thermostatic influence upon the specimens.

4. Results

Throughout this presentation of results we shall employ plots of $\log\theta$ against $\log\dot{c}$, these quantities being derived from raw data using Equations 1 and 5 as previously explained. It will also be remembered that, on such a plot, a change of θ_0 without change in $\log\Phi$ produces a simple vertical diplacement of data along the $\log\theta$ axis.

4.1. Typical results for NR adhesive and glass substrate

Fig. 4 presents extensive typical data for a particular formulation containing 7% by weight of artificial sebum, all testing being carried out at 23 ± 2°C. The system is denoted (NR/7% sebum/glass).

Hard-machine data are shown by points with vertical error bars, these bars comprehending the oscillations of peel force observed in the test. These data were supplemented by dead-load tests in which 90° peel occurred under a fixed dead load. Such data are shown with horizontal error bars to indicate fluctuations in the rate of peel. Finally, soft-machine data are shown as individual points without error bars, since with this method there are no fluctuations. A number of features are immediately apparent.

1. The conventional hard-machine and dead-load results define an almost linear upper-bound

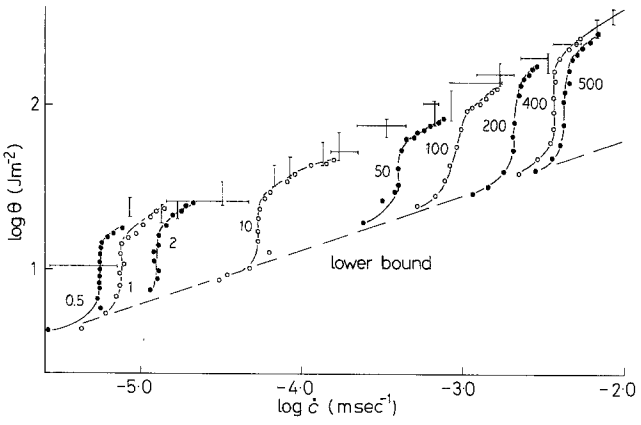

Figure 4 Collected data for peeling energy against peeling speed. NR + 7% sebum at 23° C peeled from a glass substrate. Points give soft-machine data with cross-head speed in mm min^{-1} shown by numbers. Vertical error bars give hard-machine data. Horizontal error bars give dead-load data.

relationship between log θ and log $\dot{c}$. The increase in θ with peeling speed is normal with rubber-like adhesives and reflects increasing viscoelastic energy dissipation with rising rate of test. The hard-machine and dead-load data are in good agreement.

2. By contrast, the soft-machine data reveal a wealth of detail. Although in each individual test the peeling energy θ does eventually "climb" on to the upper-bound curve defined by the hard-machine and dead-load tests, many points fall systematically below this upper-bound. Where they do follow the upper-bound, the soft-machine θ values correlate with the lower end of the hard-machine error bars.

3. In each soft-machine test the θ values at first lie on a *lower-bound* curve (shown dotted) which is roughly parallel to the upper bound but is displaced downwards by a factor of about 3. Although upper and lower bounds are not exactly parallel this suggests that both are controlled by the same function $\Phi(\dot{c})$ but that either θ_0 or some other factor differs between the bounds.

4. In each soft-machine test, after a certain amount of peeling has occurred, there is a transition from the lower to the upper bound which takes place at constant $\dot{c}$. We shall call this "critical" value $\dot{c}^*$. In some tests the transition is less abrupt, being spread over a range of peeling speeds.

5. The particular velocity $\dot{c}$ at which the transition occurs is a function of cross-head speed $\dot{X}$.

6. It should be made clear that the form of the curves in Fig. 4 cannot be explained as an artefact due to stretching of the peeled portion of the strip or slack in the trolley arrangement. The extension of the backing cloth under the highest loads encountered never exceeds 5% of its length. Thus the true rate of peel can only differ from that predicted by Equation 5 by 5% at the most. (Deflection of the trolley affords negligible errors of the order of 0.1%.) The maximum combined errors are less than the experimental scatter.

4.2. Effects of adhesive thickness or loading

Using the same system (Nr/7% sebum/glass at 22° C) the dry weight of adhesive per unit area of cloth was varied between 0.1 and 1 kg m^{-2}. The results are shown in Fig. 5 for a cross-head speed of 50 mm min^{-1}. In Fig. 6 two quantities are plotted logarithmically against the weight of adhesive, namely the peel velocity $\dot{c}^*$ at which the lower-to-upper bound transition occurs (circles) and the upper-bound θ value at an arbitrary peel velocity of log $\dot{c} = -3.1$ where $\dot{c}$ is measured in m sec^{-1}. The log θ plot shows both soft-machine data (crosses) and hard-machine

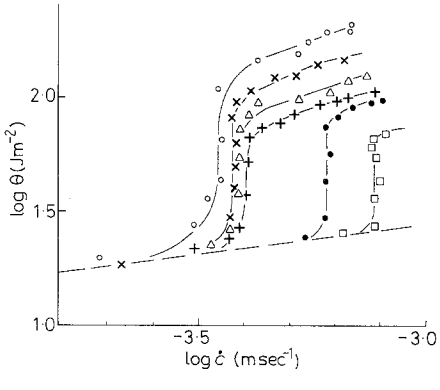

Figure 5 Effect of adhesive loading (thickness) on the soft-machine data. Weights in g m^{-2} are (○) 942, (×) 332, (△) 309, (+) 215, (●) 149, (□) 107.

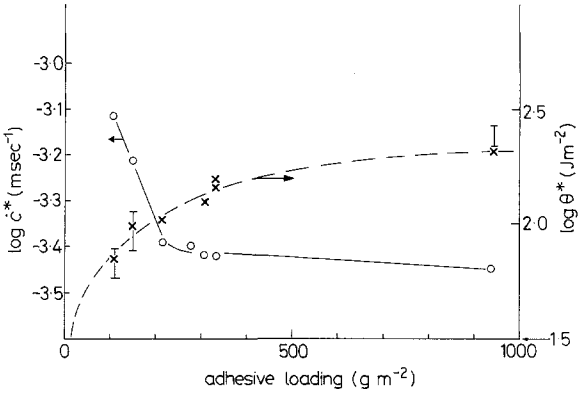

Figure 6 Effect of adhesive loading on transition velocity and on peeling energy at log $\dot{c} = -3.1$ (denoted θ^*). Error bars give hard-machine data for θ^*.

data (error bars) and these agree very well. The transition velocity $\dot{c}^*$ is strongly dependent on loading at low loadings, but becomes virtually independent of loading above about 0.3 kg m^{-2}. The upper bound θ value also varies most rapidly at low loadings, tending to constancy at high loadings. The increase in θ with loading is similar to that observed by other workers. The fall in $\dot{c}^*$ with loading is, of course, unique to soft-machine testing and has not, therefore, been reported previously.

4.3. Effects of spring stiffness

Fig. 7 shows that at constant $\dot{X}$ spring stiffness affects the transition velocity $\dot{c}^*$ but not the upper or lower bound values of θ. As the spring stiffness decreases (as k increases), $\dot{c}^*$ is reduced and the transition itself tends to broaden.

This effect can be rationalized by considering the rate of load application $\mathrm{d}P/\mathrm{d}t$, since

$$\frac{\mathrm{d}P}{\mathrm{d}t} = \frac{1}{k}\frac{\mathrm{d}L}{\mathrm{d}t} = \frac{1}{k}(\dot{X} - \dot{c}) \qquad (6)$$

A plot of $\dot{P}$ against $\dot{c}^*$ for the (NR/7% sebum/glass) system at 22° C is shown as the lowest of the curves in Fig. 8, and reveals a single linear relationship for different cross-head speeds and spring constants. This plot shows clearly that the effects on transition speed $\dot{c}^*$ of *both* spring stiffness *and* cross-head speed are due to a single parameter, namely the rate-of-loading $\dot{P}$.

Just as higher $\dot{X}$ means higher $\dot{P}$ at fixed spring constant, so an increase in spring stiffness at constant $\dot{X}$ gives rise to a high loading rate. The data thus show that

$$\dot{c}^* = \alpha'\dot{P} \qquad (7)$$

since $\theta = P/b$ for 90° peel, we can rewrite this

$$\dot{c}^* = \dot{\theta} \qquad (8)$$

and α then has the dimensions of reciprocal energy density.

Fig. 8 also shows data for other NR systems namely (NR/glass at 25° C), (NR/skin at 25° C) and (NR/skin at 37° C), all plotted as $\dot{P}$ against $\dot{c}^*$. All systems display linearity on this plot but α varies from system to system.

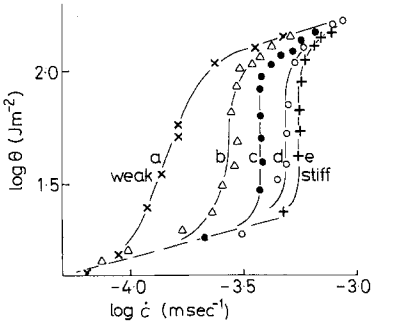

Figure 7 Effect of spring stiffness on soft-machine data. Inverse spring constants k (in units of 10^{-2} m N^{-1}) are (a) 11.00, (b) 8.56, (c) 5.09, (d) 2.26, (e) 1.85.

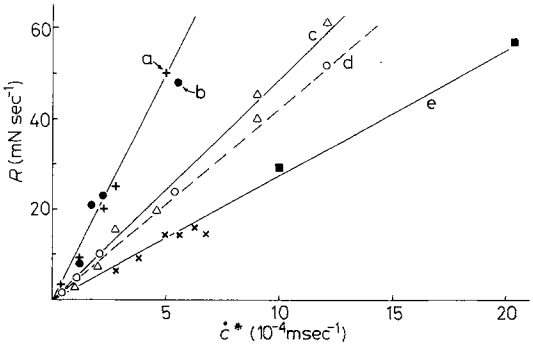

Figure 8 Plots of loading rate R against transition peel speed for various systems. (a) NR/glass/25° C; (b) NR/skin/25° C; (c) NR/skin/37° C; (d) AR/3.58% linoleic acid/glass/23° C; (e) NR/7% sebum/glass 23° C. For (e) crosses show different springs, and squares different cross-head speeds.

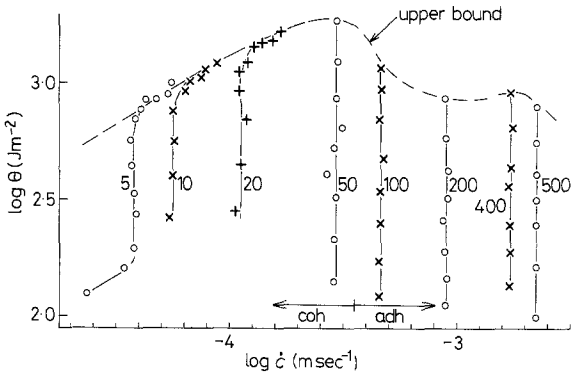

Figure 9 Soft machine data for acrylic adhesive, (AR/3.58% linoleic acid/glass/23° C at various cross-head speeds in mm min^{-1}.

4.4. Typical results for acrylic rubber adhesive

Unlike the NR adhesive, the acrylic rubber adhesive (AR) exhibits peaks in the curve of log θ against log $\dot{c}$ when tested on a hard machine. Typical soft machine data is shown in Fig. 9 for the system (AR/3.58% linoleic acid/glass at 23° C). It is evident that the general features found in soft-machine testing of NR systems are preserved but that a new effect is also found. That is, in regions where the upper envelope shows decreasing θ with increasing $\dot{c}$, the soft-machine test takes place at essentially constant peeling velocity $\dot{c}^*$ up to some critical force. At peak force (peak θ) peeling in these tests becomes unstable and the peel strip is removed very rapidly from the substrate. It is, in fact, possible to resolve the decaying force–time curve in this unstable region where peel velocity exceeds the cross-head speed. The results of one such analysis is shown in Fig. 10, where log θ against log $\dot{c}$ data are shown for (AR/1.79% linoleic acid/glass at 23° C) at several cross-head speeds. Data points up to the peak in the force–time curve are shown as crosses and echo the results already shown in Fig. 9. The peak θ values for various cross-head speeds are shown as filled circles. Data points derived from the negative slope force–time curve beyond the peak, are shown by other symbols while the arrow on the line connecting these points indicates increasing time.

What happens at the peak is that peeling accelerates so rapidly that $\dot{c}$ jumps by a factor of about 100 from Point A in Fig. 10 to Point B, before stabilizing. The failure energy then drops slightly to C at constant (high) velocity before tracing out the reducing velocity pathway C → D. This pathway passes precisely through the peak points from higher cross-head speeds (filled circles in Fig. 10), and may thus be considered a true upper-bound curve. The hard-machine data for this system shows significant scatter but are otherwise consistent with the upper bound defined, rather precisely, by the soft-machine tests.

It is typical of AR adhesives that they exhibit a second type of transition, namely a cohesive–adhesive transition. This is indicated in Fig. 9 by the terms "coh" and "adh" respectively. As is commonly found with AR adhesives, cohesive failure predominates at low $\dot{c}$ and the transition to adhesive failure is accompanied by a decrease in θ, though not a dramatic one for the system illustrated in Fig. 9. Cohesive–adhesive transitions are also observed in NR adhesive systems

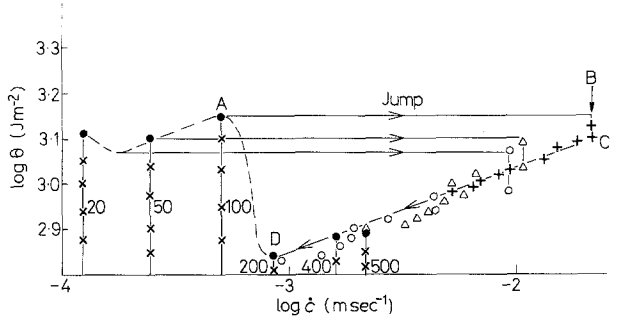

Figure 10 As Fig. 9 but for 1.79% linoleic acid, showing analysis of force–time curve beyond its peak. Arrows indicate increasing time and filled circles show force–time maxima at various cross-head speeds in mm min^{-1}.

but at much lower velocities and without sudden changes in θ.

5. Discussion

It has not been our purpose in this paper to present exhaustive and systematic results for the wide range of systems (adhesive/additive/substrate/temperature) that has been studied to date. Such a presentation will be reserved for a future publication. We have rather described typical data that exemplify the soft-machine peel test and allow us to compare results obtained by this technique with those afforded by conventional hard-machine or dead-load tests.

For uncrosslinked adhesives we have seen that soft-machine tests give information that cannot be derived from conventional tests. In particular they reveal the existence of a lower-bound in the log θ against log $\dot{c}$ plot, together with a lower-to-upper bound transition occurring at a peel velocity $\dot{c}^*$ that is sensitive to several variables. These variables are cross-head speed, adhesive thickness, spring constant and temperature, as well of course as adhesive composition. Some of these effects can be rationalized in terms of the rate-of-loading variable which depends on both cross-head speed and spring stiffness.

Before attempting to explain the special features of soft-machine testing it is instructive to note that highly analogous data have been obtained by Döll *et al.* [23] in a study of crazing in glassy polymers. Fig. 11 shows their results for craze width (opening displacement) against crack speed in fatigue tests at different frequencies. These data bear a strong resemblance to our results for θ against $\dot{c}$, showing an upper bound which corresponds to dead loading, a lower bound, and a transition between the bounds which moves to higher crack velocity as the frequency (and thus the loading rate) increases.

We believe the similarity between our results and those of Döll *et al.* is not accidental. For craze opening in the work of Döll *et al.* represents the degree of bluntness of the crack, while it is known that fracture energy (and, by implication, adhesive failure energy) in rubber-like solids can be written [24]

$$\theta \simeq W_b D \tag{9}$$

so that

$$\log \theta = \log W_b + \log D \tag{10}$$

where D is the crack tip diameter (bluntness) and W_b is the energy density to tensile failure. There is therefore a direct connection between θ and "crack bluntness". In particular, increasing bluntness at constant W_b will cause a vertical shift of log θ data creating a lower-to-upper bound transition.

Furthermore, until peel rate reaches very high values, the failure of an uncrosslinked adhesive in peel is craze-like. That is, the rubber fibrillates into filaments which then either fail plastically in tension (cohesive failure) or else pull free of the substrate (adhesive failure). The analogy between crazing at a crack tip in a brittle solid, and bond failure in peeling is therefore reasonable.

We propose that lower-bound failure represents peel propagation with a "sharp crack", that is, a peel front at which stress is highly concentrated. This type of peeling would correspond to that obtained in crosslinked rubbers where no plastic mechanism for crack blunting exists. Such failure would be insensitive to adhesive layer thickness and this is indeed the case for lower-bound peel.

As force increases, however, uncrosslinked adhesives begin to flow. This results in a blunt-

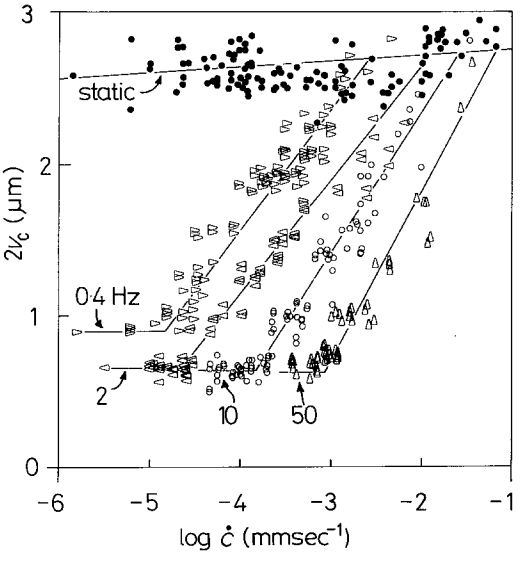

Figure 11 Data of Döll *et al.* [23] showing craze opening displacement in polymethyl methacrylate as a function of crack speed at different frequencies of fatigue loading (in Hz). Note upper and lower bounds and rate-sensitive transition analogous to Fig. 4. (Reproduced from *Polymer* **24** (1983) 1216, by permission.)

ing of the "crack" or peel front, that is a dispersal of stress concentration. A larger volume of material at the tip is subjected to high strain and the peeling energy rises accordingly. The degree of crack blunting is limited (a) by the total layer thickness and (b) by the removal of flowing material as the crack propagates and "renews" its tip. In consequence of (a), the upper-bound θ value increases with adhesive layer thickness while because of (b) the onset of crack blunting is delayed by rapid load application (less flow occurs before the crack propagates).

This sharp crack/blunt crack model seems capable therefore of providing a qualitative explanation of our soft-machine results on uncrosslinked adhesives, as well as the results of Döll *et al.* on craze zones at crack tips in rigid plastics. It remains for us to translate this qualitative model into a quantitative mathematical theory which will define the role of material parameters such as viscosity, intrinsic adhesion and temperature dependence.

The reason why lower-bound data are not observed in hard-machine testing is probably that the rise of peel force from zero to its "steady state" value is always ignored and only the steady state peel force measured. We suggest that the "information" on lower bound and transition phenomena is contained in the initial rise of force in a hard machine test. These effects *do* therefore appear in such tests but are ignored. Even now, however, it is possible to recognize certain practical advantages in the 'soft-machine' testing of these types of adhesive. These can be summarized as follows.

1. A single soft-machine test provides data over a *range* of peeling speeds and thus saves testing time.

2. Soft-machine tests provide *new* information such as the lower-bound behaviour of θ and the transition peel velocity $\dot{c}^*$. These new data not only provide insight into the peeling process but also may be of practical significance. Lower-bound θ, for example, may be far more relevant to low-severity adhesive failure such as that encountered in the use of surgical adhesives, than the upper-bound θ normally measured in peel tests. Since upper bound θ may in some cases exceed lower bound θ by a factor of 30, this is a matter of vital concern. Likewise the linear dependence of $\dot{c}^*$ upon loading rate (Fig. 8) seems to be linked to the rheological properties of the adhesive and may therefore help to characterize these properties.

3. Because of the sensitivity of $\dot{c}^*$ and $\Delta\theta$ (lower to upper bound) to factors such as thickness and rheology, the soft-machine test should prove particularly valuable as a quality control test in the manufacture of pressure sensitive adhesive products.

Acknowledgements

Thanks are due to the Science and Engineering Research Council for a research grant and to Smith and Nephew Research Ltd, for supplying adhesives and for helpful discussion. We are also grateful to Dr W. Döll for permission to reproduce the data shown in Fig. 11.

References

1. J. J. BIKERMAN, "The Science of Adhesive Joints", 2nd Edn. (Academic Press, New York, 1968).
2. A. N. GENT and G. R. HAMED, *Polym. Eng. Sci.* **17** (1977) 462.
3. J. O. HENDRICKS and C. A. DAHLQUIST, "Adhesion and Adhesives", Vol. 2, edited by R. Hovwink and G. Salomon (Elsevier, Amsterdam, 1967).
4. A. J. DUKE, *J. Appl. Polym. Sci.* **18** (1974) 3019.
5. D. H. KAELBLE, "Physical Chemistry of Adhesion", edited by D. H. Kaelble (Wiley International, 1979).
6. D. SATAS, "Handbook of Pressure Sensitive Adhesive Technology", edited by D. Satas (Van Nostrand Reinhold, New York, 1982).
7. E. H. ANDREWS and A. J. KINLOCH, *Proc. R. Soc. A.* **332** (1973) 385.
8. A. N. GENT and J. SCHULTZ, *J. Adhesion* **3** (1972) 281.
9. K. KENDAL, *J. Phys. D. Appl. Phys.* **4** (1971) 1186.
10. D. MAUGIS and M. BARQUINS, *ibid.* **11** (1978) 1989.
11. M. BARQUINS, *Int. J. Adhesion Adhesives* **3** (1983) 71.
12. A. N. GENT and A. J. KINLOCH, *J. Polym. Sci. A2* **9** (1971) 659.
13. E. H. ANDREWS, *J. Mater. Sci.* **9** (1974) 887.
14. A. AHAGON and A. N. GENT, *J. Polym. Sci. Polym. Phys. Ed.* **13** (1975) 1285.
15. G. J. LAKE and A. STEVENSON, "Adhesion 6", edited by K. W. Allen (Applied Science, Barking, 1982) p. 41.
16. G. J. LAKE and A. G. THOMAS, *Proc. R. Soc. A* **300** (1967) 108.
17. N. E. KING and E. H. ANDREWS, *J. Mater. Sci.* **13** (1978) 1291.
18. G. J. LAKE and P. B. LINDLEY, *J. Appl. Polym. Sci.* **9** (1965) 1233.
19. D. H. KAELBLE, *Trans. Soc. Rheol.* **4** (1960) 45.
20. A. N. GENT and R. PETRICH, *Proc. R. Soc. A*

310 (1969) 433.
21. D. W. AUBREY, "Developments in Adhesives I", edited by W. C. Wake (Applied Science, Barking, 1977) p. 127.
22. D. SATAS and R. MIHALIK, *J. Appl. Polym. Sci.* **12** (1968) 2371.
23. W. DÖLL, L. KÖNCZÖL and M. G. SCHINKER, *Polymer* **24** (1983) 1213.
24. A. G. THOMAS, *J. Polym. Sci.* **18** (1955) 177.

Received 27 July
and accepted 20 November 1984